Synthesis of Zirconium Pinacolate and Mechanism of Its Thermal Transformation to ZrO_2: Impact of a Vicinal Diol Ligand

Cecilia A. Zechmann, Kirsten Folting, and Kenneth G. Caulton*

Department of Chemistry and the Molecular Structure Center, Indiana University, Bloomington, Indiana 47405-4001

Received September 24, 1997. Revised Manuscript Received June 23, 1998

Reaction of $Zr_2(O^iPr)_8(HO^iPr)_2$ with a slight excess of pinacol ($HOCMe_2CMe_2OH$) yields $Zr_2(OCMe_2CMe_2O)_2(OCMe_2CMe_2OH)_4$, as confirmed by X-ray crystallography. Inter- and intramolecular hydrogen bonding results in the polymeric solid-state structure and the subsequent nonvolatility and reduced solubility of the species. The thermal transformation of zirconium pinacolate occurs in two distinct steps, as seen by the thermal gravimetric analysis (TGA), and occurs at <300 °C, yielding ZrO_2, as determined by X-ray powder diffraction. GC−MS analysis of the thermolysis byproducts reveals six species: pinacol, pinacolone, 2,3-dimethyl-2-butene (tetramethylethylene) (trace amounts), 2,3-dimethyl-butadiene (DMBD), 2,3-dimethyl-3-buten-2-ol (DMB-ol), 2,2,5,6,6-pentamethyl-4-hepten-3-one (PMH), and 1,3,5-tri-*tert*-butylbenzene (TTB). Real-time monitoring of the thermal transformation is achieved by carrying out the experiment inside a mass spectrometer. This novel experiment confirms that while only pinacol is lost in step I, step II consists of two phases. In step IIA, pinacolone, DMB-ol, PMH, and TTB are evolved, while in step IIB, only pinacolone and DMBD are formed. The observations support a primary mechanism for the formation of all C_6 products except DMBD, which is a dehydration product of pinacolone. Mechanistic studies involving isotopic labeling experiments suggest that the C_{12} and C_{18} products are formed by a secondary process involving the interaction of evolved pinacolone with the metal oxide species. Crystallographic data ($P\bar{1}$/−169 °C) for $Zr_2(OCMe_2CMe_2O)_2(OCMe_2CMe_2OH)_4$ are as follows: $a = 21.2305(5)$ Å, $b = 22.905(5)$ Å, $c = 10.508(3)$ Å, $\beta = 104.01(1)°$, with $Z = 2$.

Introduction

The unique physical and electrical properties of many metal oxides has resulted in an ever-increasing demand for their production.[1] As refractory materials, their brittle nature has led to the implementation of solution- and vapor-phase synthetic methodologies, especially in the construction of thin films suitable for industrial applications. Among the more widely used techniques are metal organic decomposition (MOD), metal organic chemical vapor deposition (MOCVD), plasma enhanced chemical vapor deposition (PECVD), and gel techniques and sputtering.[2] All of these methods (except sputtering) share the need for a volatile or soluble precursor compound, and as a result, precursor synthesis and design continue to be active and expanding areas of research.[3,4]

While much work has been done on the mechanisms involved in sol−gel technologies,[2b,5,6] only a limited number of mechanistic studies have been reported on the thermal transformations of metal alkoxides.[7−11] As all existing methodologies require heating at some point, it follows that any new mechanistic information in this area may have broad applications. As the past studies

(1) (a) Rao, C. N. R.; Raveau, B. *Transition Metal Oxides*; VCH Publishers: New York, 1995. (b) West, A. R. *Solid State Chemistry and its Applications*; Wiley: New York, 1984. (c) Sanders, H. J. *Chem. Eng. News* **1984**, *62*, 2(28), 26. (d) Ryshkewitch, E. *Oxide Ceramics*; Academic Press: New York and London, 1960.

(2) Marshall, J. M.; Kirov, N.; Vavrek, A.; Maud, J. M., Eds.; *Future Directions in Thin Film Science and Technology*; World Scientific: Singapore, 1997. (b) Brinker, C. J.; Scherer, G. W. *Sol−Gel Science: The Physics and Chemistry of Sol−Gel Processing*; Academic Press: San Diego, 1990. (c) Klemperer, W. G.; Mainz, V. V.; Ramamurthi, S. D.; Rosenberg, R. S. In *Better Ceramics through Chemistry. III*; Brinker, C. J.; Clark, D. E.; Ulrich, D. R., Eds.; North-Holland: New York, 1988. (d) *Science of Ceramic Chemical Processing*; Hench, L. L.; Ulrich, D. R.; Eds.; Wiley: New York, 1984.

(3) For a thorough introduction, see: (a) Bradley, D. C.; Mehrotra, R. C.; Gaur, D. P. *Metal Alkoxides*; Academic Press: London, 1978. (b) Caulton, K. G.; Hubert-Pfalzgraf, L. G. *Chem. Rev.* **1990**, *90*, 969.

(4) Veith, M.; Mathur, S.; Mathur, C. *Polyhedron* **1998**, *17*, 1005. (b) Hubert-Pfalzgraf, L. G. *New J. Chem.* **1995**, *19*, 727. (c) Mehrotra, R. C.; Singh, A.; Sogani, S. *Chem. Soc. Rev.* **1994**, 215. (d) Mehrotra, R. C.; Singh, A.; Sogani, S. *Chem. Rev.* **1994**, *94*, 1643.

(5) For example, see: (a) Stacey Fu, C. Y.; Lackritz, H. S.; Priddy, D. B., Jr.; McGrath, J. E. *Chem. Mater.* **1996**, *8*, 514. (b) Rai, J.; Mehrotra, R. C. *J. Non-Cryst. Solids* **1993**, *152*, 118.

(6) For a recent review, see: Narendar, Y.; Messing, G. L. *Catalysis Today* **1997**, *35*, *3*, 247.

(7) Hubert-Pfalzgraf, L. G. *New J. Chem.* **1987**, *11*, 663−675. (b) Bradley, D. C.; Mehrotra, R. C.; Gaur, D. P. *Metal Alkoxides*; Academic Press: London, 1978. (c) Bradley, D. C. *Chem. Rev.* **1989**, *89*, 1317−1322.

(8) Xue, Z.; Vaartstra, B. A.; Caulton, K. G.; Chisholm, M. H. *Eur. J. Solid State Inorg. Chem.* **1992**, *29*, 213−225. (b) Bradley, D. C.; Faktor, M. M. *J. Appl. Chem.* **1959**, *9*, 435−439. (c) Bradley, D. C.; Faktor, M. M. *Trans. Faraday Soc.* **1950**, *55*, 2117−2123.

(9) Stecher, H. A.; Sen, A. *Inorg. Chem.* **1989**, *28*, 3280−3282.

(10) Nandi, M.; Rhubright, D.; Sen, A. *Inorg. Chem.* **1990**, *29*, 3066−3068.

(11) Jeffries, P. M.; Dubois, L. H.; Girolami, G. S. *Chem. Mater.* **1992**, *4*, 1169−1175.

S0897-4756(97)00644-3 CCC: $15.00
Published on Web 08/22/1998

have concentrated on typical monodentate alkoxide complexes, we have chosen to examine the thermal properties of a metal *di*olate (vicinal), zirconium pinacolate ($Zr/OCMe_2CMe_2O$). It is our belief that while the structure and physical properties imparted by this new ligand class will be intrinsically interesting, the thermal studies may prove to be especially valuable. By allowing for a comparison to the previous reports on traditional monodentate alkoxides, any striking similarities and/or differences may significantly advance the extent of our understanding of these processes.

Moreover, vicinal diolates offer new mechanistic possibilities. Although they have been neglected in the past for this particular application, the behavior of metal-bound vicinal diols, including thermal, has been reported and varies depending on the metal, reaction conditions, and the diol itself.[12−14] This ligand class possesses a structural feature appealing in a precursor ligand, namely, the large number of stable organic fragments which can be derived from them. Using pinacol as an example, there exists a number of possible ligand decomposition products: pinacol itself, pinacolone, 2,3-dimethyl-2-butene, and acetone, to name a few. It is our hope that the large number of possible decomposition products will correlate to several working oxide formation mechanisms and ultimately result in a relatively low thermolysis temperature. This would be especially valuable for refractory oxides such as ZrO_2, if it would lead to crystalline material at unusually low temperatures.

Experimental Section

General. All manipulations were carried out using standard Schlenk techniques or in an argon atmosphere glovebox. Hexanes, pentane, and benzene were distilled from Na/benzophenone, CH_2Cl_2 was distilled from CaH_2, and toluene was distilled from Na. All solvents were collected and stored under nitrogen prior to use. Pinacol was sublimed and stored under nitrogen. $Zr_2(O^iPr)_8(HO^iPr)_2$ was obtained from Aldrich and recrystallized from pentane/2-propanol (10%) prior to use. Acetone-d_6 was purchased from Cambridge Isotope Laboratories and used as received. NMR spectra (^1H) were recorded on a Varian Gemini 2000 or Inova 400 or Inova 500 spectrometer. Chemical shifts are referenced to residual solvent peaks. Deuterated NMR solvents were dried over $CaCl_2$ prior to use and stored under argon.

Thermolysis Studies. Thermogravimetric Analysis (TGA) studies were carried out with a Dupont Instruments 951 Thermogravimetric Analyzer using a 70 mL/min He flow rate and a 5−10 °C/min heating rate. Gas chromatography−mass spectrometry (GC−MS) data were collected using a Hewlett-Packard 5890 Series II gas chromatograph and 5971 Series mass-selective detector equipped with a 70 eV electron impact (EI) ion source. Samples for GC−MS analysis were obtained by two techniques. In the first method, the thermal transformation of the precursor was carried out on the benchtop in a double-bottomed Schlenk flask. $Zr_2(OCMe_2CMe_2O)_2(OCMe_2CMe_2OH)_4$ was loaded into one side of the flask, and a small amount of CH_2Cl_2 was added and immediately removed in vacuo to leave a thin layer of zirconium pinacolate in optimal thermal contact with the flask. The flask was evacuated and the side containing the zirconium pinacolate was heated with a Wood's metal bath to 280 °C for 30 min while the empty side was cooled with liquid nitrogen (−196 °C) to collect the organic products. Alternatively, the transformation was carried out in a tube furnace. In the latter case, the precursor was loaded into the center of a glass tube which was then heated in a furnace. The resulting transformation takes place under dynamic vacuum with a liquid nitrogen trap to capture the organic products.

Temporal Thermolysis Studies. Pyrolysis was also carried out inside a Kratos MS80 mass spectrometer equipped with a variable-temperature insertion probe. A sample capillary was loaded with a small amount of $Zr_2(OCMe_2CMe_2O)_2(OCMe_2CMe_2OH)_4$ and placed in the mass spectrometer probe. The temperature of the probe was ramped (7−10 °C/min) from room temperature to 200 °C. During this time period, step I was completed. After the total ion current returned to baseline, the temperature was further ramped (7−10 °C/min) to 270 °C. Once again, the total ion current increased as step II began and data was continuously collected until the total ion current returned to baseline.

Quantification of Volatiles. Into one lower arm of an H-shaped apparatus was placed $Zr_2(OCMe_2CMe_2O)_2(OCMe_2CMe_2OH)_4$ (0.046 g, 0.052 mmol). The vessel was evacuated and the lower arm containing the sample was submerged into a Wood's metal bath (∼90 °C). The temperature was increased to 150 °C while the vessel was under dynamic vacuum. At this point, the valve to the vacuum was closed and the chamber for collection of volatiles was submerged in a liquid nitrogen bath. The sample temperature was increased to 280 °C and held for 30 min, at which point the thermolysis was expected to be complete. The vessel was returned to 25 °C and 0.6 mL of $CDCl_3$ containing 0.0065 g of hexamethylbenzene (0.040 mmol) was added to the condensed volatiles to give a colorless solution. This solution was transferred to an NMR tube via syringe for evaluation by ^1H NMR.

Synthesis of $Zr_2(OCMe_2CMe_2O)_2(OCMe_2CMe_2OH)_4$. Into a flame-dried Schlenk flask were placed 2.41 g of $Zr_2(O^iPr)_8(HO^iPr)_2$ (3.71 mmol) and 2.71 g of $HOCMe_2CMe_2OH$ (29.6 mmol). Hexane was added (∼100 mL) to dissolve the reactants and the resulting solution was refluxed overnight, yielding a white precipitate. The mixture was filtered and the solid washed with hexanes to yield 82%. Elemental Anal. Calcd for $C_{36}H_{72}O_{12}Zr_2$: C, 48.94; H, 8.67. Found: C, 49.37; H, 8.83. ^1H NMR ($C_2D_2Cl_4$, 65 °C): 1.38 (s), 1.29 (s), 1.15 (s), 1.05 (s) ppm.

Synthesis of $Zr_2(OCMe_2CMe_2O)_2(OCMe_2CMe_2OH)_4$-$d_{72}$. The deuterated analogue was prepared in a similar fashion, by substituting pinacol-d_{12} for perprotio pinacol. The pinacol-d_{12} was prepared using a reported literature[15] procedure, by substituting acetone-d_6. The isotopically labeled pinacol was dried prior to use, first by azeotropic distillation of H_2O with benzene, followed by sublimation and storage in an argon-atmosphere glovebox.

X-ray Structure Determination of $2Zr_2(OCMe_2CMe_2O)_2(OCMe_2CMe_2OH)_4$:1.5$C_6H_6$:0.5$C_6H_{14}$. A solution of $Zr_2(O^iPr)_8(HO^iPr)_2$ in hexanes was layered over a benzene solution of 8 equiv of pinacol. This unstirred reaction is complete in 1 week. A suitable single crystal was selected from the bulk sample and affixed to a glass fiber using silicone grease. The crystal was then transferred to the goniostat, where it was cooled to −169 °C, for characterization and data collection. Crystallographic data are summarized in Table 1. A systematic search of a limited hemisphere of reciprocal space yielded a set of reflections which exhibited no symmetry other than $\bar{1}$ and no systematic extinctions. The choice of the centrosymmetric space group $P\bar{1}$ (No. 2) was confirmed by the subsequent solution and refinement of the structure. The residual for the averaging of 1623 intensities observed more than once was 0.024. Plots of the four standard reflections measured every 400 reflections showed no significant trends. No absorption

(12) Olivier, M.; Villiers, C.; Ephritikhine, M. *Angew. Chem., Int. Ed. Engl.* **1996**, *35*, 1129−1130.

(13) Chisholm, M. H.; Parkin, I. P.; Streib, W. E.; Eisenstein, O. *Inorg. Chem.* **1994**, *33*, 812−815.

(14) Hermann, W. A.; Watzlowik, P. *J. Organomet. Chem.* **1992**, *441*, 265−270. (b) Gable, K. P.; Juliette, J. J. *J. Am. Chem. Soc.* **1995**, *117*, 955−962.

(15) Gilman, H. In *Organic Syntheses*; Blatt, A. H., Ed.; John Wiley and Sons: New York, 1952, pp 459−462.

Table 1. Crystallographic Data

formula	$2*[C_{36}H_{74}O_{12}Zr_2]:1.5C_6H_6:0.5C_6H_{14}$		
a, Å	21.2305(5)	space group	$P\bar{1}$
b, Å	22.905(5)	*T*, °C	−169
c, Å	10.508(3)	*λ*, Å	0.71069
β, Å	104.01(1)	ρ_{cald}, g/cm^{-3}	1.292
V, Å^3	4942.85	μ(Mo Kα), cm^{-1}	4.6
Z	2	R	0.0637
formula weight	1923.09	R_w	0.0672

Table 2. Selected Distances (Å) and Angles (deg) for $Zr_2((OC(CH_3)_2C(CH_3)_2O)_2((OC(CH_3)_2C(CH_3)_2OH)_4$

Distances

Zr(1)···Zr(2)	3.5194(13)	Zr(2)−O(14)	2.039(5)
Zr(1)−O(3)	2.199(5)	Zr(2)−O(35)	2.001(5)
Zr(1)−O(6)	1.978(5)	Zr(2)−O(38)	2.333(5)
Zr(1)−O(11)	2.148(5)	Zr(2)−O(43)	1.936(5)
Zr(1)−O(19)	2.206(5)	O(19)···O(30)	2.550(7)
Zr(1)−O(22)	2.089(5)	O(22)···O(38)	2.656(7)
Zr(1)−O(27)	1.963(5)	O(14)···O(46)	2.795(7)
Zr(2)−O(3)	2.145(5)	O(30)A···O(46)B	2.689(7)
Zr(2)−O(11)	2.197(5)	O(30)B···O(46)A	2.700(7)

Angles

Zr(1)−O(3)−Zr(2)	108.23(20)	Zr(1)−O(11)−Zr(2)	108.21(20)
Zr(1)−O(3)−C(28)	163.7(5)	Zr(2)−O(43)−C(44)	165.2(5)
O(3)−Zr(1)−O(6)	73.43(19)	O(11)−Zr(2)−O(14)	74.18(18)
O(3)−Zr(1)−O(11)	71.03(18)	O(11)−Zr(2)−O(3)	71.13(17)
O(11)−Zr(1)−O(19)	116.66(19)	O(3)−Zr(2)−O(35)	108.67(19)
O(19)−Zr(1)−O(6)	99.99(20)	O(35)−Zr(2)−O(14)	103.80(20)
O(22)−Zr(1)−O(3)	89.56(19)	O(38)−Zr(2)−O(11)	78.27(18)
O(22)−Zr(1)−O(6)	100.24(21)	O(38)−Zr(2)−O(14)	94.40(19)
O(22)−Zr(1)−O(11)	89.08(19)	O(38)−Zr(2)−O(3)	84.24(18)
O(22)−Zr(1)−O(19)	70.13(19)	O(38)−Zr(2)−O(35)	70.33(19)
O(27)−Zr(1)−O(3)	120.91(19)	O(43)−Zr(2)−O(11)	113.78(19)
O(27)−Zr(1)−O(6)	94.13(20)	O(43)−Zr(2)−O(14)	91.79(20)
O(27)−Zr(1)−O(11)	95.69(19)	O(43)−Zr(2)−O(3)	96.80(19)
O(27)−Zr(1)−O(19)	80.52(19)	O(43)−Zr(2)−O(35)	97.80(21)
O(27)−Zr(1)−O(22)	149.07(20)	O(43)−Zr(2)−O(38)	167.63(19)
O(3)−Zr(1)−O(19)	157.49(18)	O(3)−Zr(2)−O(14)	144.83(18)
O(6)−Zr(1)−O(11)	143.13(19)	O(11)−Zr(2)−O(35)	148.34(20)
Zr(1)−O(27)−C(28)	163.7(5)	Zr(2)−O(43)−C(44)	165.2(5)

correction was performed. The structure was solved by a combination of direct methods and difference Fourier techniques. The four Zr atoms were located in successive iterations of least-squares refinement and difference Fourier maps. At the end of the full-matrix least-squares refinements, almost all of the peaks in the difference map could be interpreted as hydrogen atoms on carbon atoms. However, space limitations in the least-squares program did not allow inclusion of the hydrogen atoms. All of the atoms were refined using anisotropic thermal parameters. Due to the large number of variables, the refinement was carried out in a cyclic manner. The final difference map was essentially featureless. All residual peaks could be interpreted as possible hydrogen atoms. Results are shown in Table 2 and Figure 1.

Results and Discussion

Synthesis of $Zr_2(OCMe_2CMe_2O)_2(OCMe_2CMe_2OH)_4$. The addition of a slight excess of pinacol (8 equiv) to $Zr_2(O^iPr)_8(HO^iPr)_2$, followed by reflux in hexanes overnight, yielded a white precipitate. X-ray crystallography identified the product as $Zr_2(OCMe_2CMe_2O)_2(OCMe_2CMe_2OH)_4$. Elemental analysis was consistent with this formulation. The room temperature ^{1}H NMR reveals several broad signals from 1.5 to 1.0 ppm. However, at higher temperature (65 °C), the ^{1}H NMR spectrum simplifies to four singlets in the methyl region, possessing approximate 1:2:2:1 relative intensities.[16]

(16) An explanation for the observed ^{1}H NMR can be found in the Supporting Information.

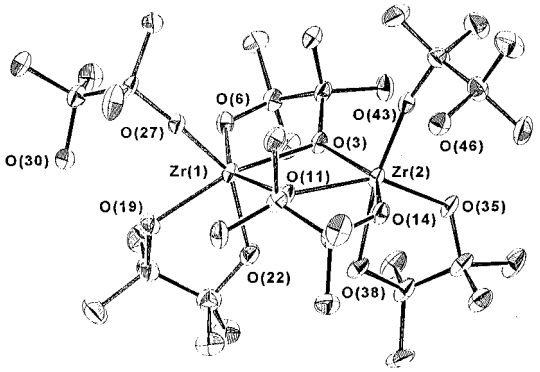

Figure 1. ORTEP representation of $Zr_2(OCMe_2CMe_2O)_2(OCMe_2CMe_2OH)_4$, showing 50% probability ellipsoids.

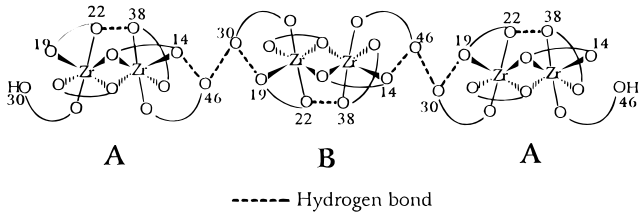

Figure 2. Schematic representation of hydrogen bonding in $Zr_2(OCMe_2CMe_2O)_2(OCMe_2CMe_2OH)_4$.

Attempts to sublime the material were unsuccessful (10^{-2} Torr, 150 °C).

Solid-State Structure of $Zr_2(OCMe_2CMe_2O)_2(OCMe_2CMe_2OH)_4$. $2Zr_2(OCMe_2CMe_2O)_2(OCMe_2CMe_2OH)_4:1.5C_6H_6:0.5C_6H_{14}$ crystallized in the centrosymmetric space group $P\bar{1}$. The asymmetric unit contains two discrete metal complexes (one is shown in Figure 1), one and one-half benzene molecules, and one-half a hexane molecule. These discrete metal complexes have identical numbering schemes but are distinguished by suffixes (A and B). The structure discussion will involve just one molecule since they display no significant differences. Although the dinuclear complex has no rigorous crystallographic symmetry, it does possess an idealized C2 axis which bisects a line joining the two bridging oxygens. The molecule has an edge-shared bioctahedral structure with significant distortions due to the ligation of chelating ligands possessing a bite angle less than 90°. The average Zr−O distance is 2.103 Å with the shortest distance involving the metal-bound oxygens of the terminal/monodentate pinacolates [O(27) and O(43)]. Two additional ligand binding modes are exhibited in this molecule. Three of the coordination sites on each metal are taken up by two bridging/chelating pinacolates, while the remaining two are occupied by terminal/chelating pinacolates.

To satisfy the oxidation state of the metals, each molecule must possess four hydroxyl protons. Two of these protons obviously belong to the pendant hydroxyl groups while some speculation remains as to the exact location of the remaining protons. Possible locations were determined by O···O distances (see Table 2 for the four shortest distances) and include O(22), O(38), O(14), and O(19). Due to lengthened Zr−O bond distances, the proton positions are proposed to be O(19) and O(38). Significant intra- and intermolecular hydrogen bonding due to the presence of the hydroxyl groups gives the solid a polymeric superstructure. Intramolecular hydrogen bonding between the axial oxygens, O(22) and

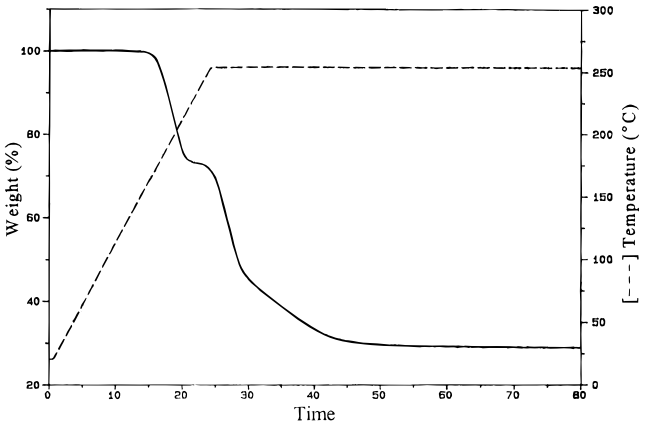

Figure 3. TGA profile of $Zr_2(OCMe_2CMe_2O)_2(OCMe_2CMe_2OH)_4$.

O(38), results in a significant distortion from octahedral geometry. This distortion primarily entails a bending out of the monodentate ligands toward the outside of the molecule along the Zr−Zr axis so that the O(27)−Zr(1)−Zr(2) and O(43)−Zr(2)−Zr(1) angles are substantially greater than 90°, allowing for the formation of a linear polymeric structure, as seen in Figure 2. The dangling hydroxyl functionality of one molecule is involved in hydrogen bonding to an oxygen of a chelating ligand on the same molecule and to the pendant hydroxyl group of its neighbor, the symmetrically independent molecule of the unit cell [i.e., O(30)A hydrogen bonds to O(19)A (2.550 Å) and O(46)B (2.689 Å)].

The zirconium pinacolate showed reduced solubility as well as volatility in comparison to its parent isopropoxide. It appears to be insoluble in aliphatic and aromatic hydrocarbons, but is soluble in chlorocarbons and Lewis basic solvents such as THF. Due to the lack of volatility (most likely the result of intermolecular hydrogen bonding) of the dinuclear zirconium pinacolate, chemical vapor deposition (CVD) studies are not possible. However, the lack of volatility does allow for bulk thermolysis as well as the implementation of a variety of novel mechanistic studies which would have been more difficult or impossible with a volatile precursor.

Solid-State Thermolysis Studies. Initial TGA studies of $Zr_2(OCMe_2CMe_2O)_2(OCMe_2CMe_2OH)_4$ revealed that upon reaching a temperature of 260−270 °C, the material decomposes within 1 h to give an off-white powder and a final weight corresponding closely to that calculated for the formation of ZrO_2 (27.9/28.4). X-ray powder diffraction studies confirmed the identity of the product as ZrO_2 (process temperature 350 °C) and revealed that there were three different phases present, the cubic, tetragonal, and baddeleyite phases, with the most abundant corresponding to the cubic phase. Unlike results reported by Xue, et al.,[8a] increasing the thermolysis temperature and/or annealing at temperatures of up to 1000 °C did not alter the phase of the resulting material or the degree of crystallinity.

Figure 3 shows the TGA profile of $Zr_2(OCMe_2CMe_2O)_2(OCMe_2CMe_2OH)_4$. The experiment was carried out using a ramp rate of 10 °C/min from room temperature to 260 °C and then holding the temperature constant (at 260 °C) until weight loss was no longer

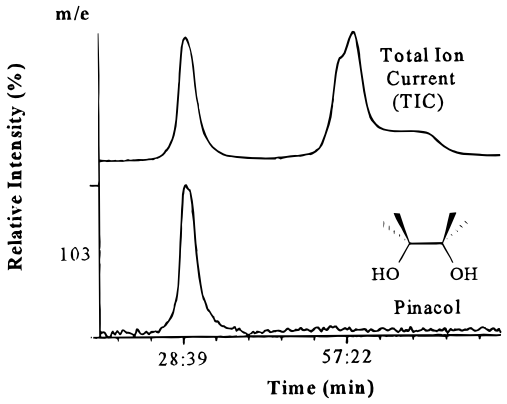

Figure 4. Total ion current (above) and selected ion chromatogram for pinacol (m/e = 103).

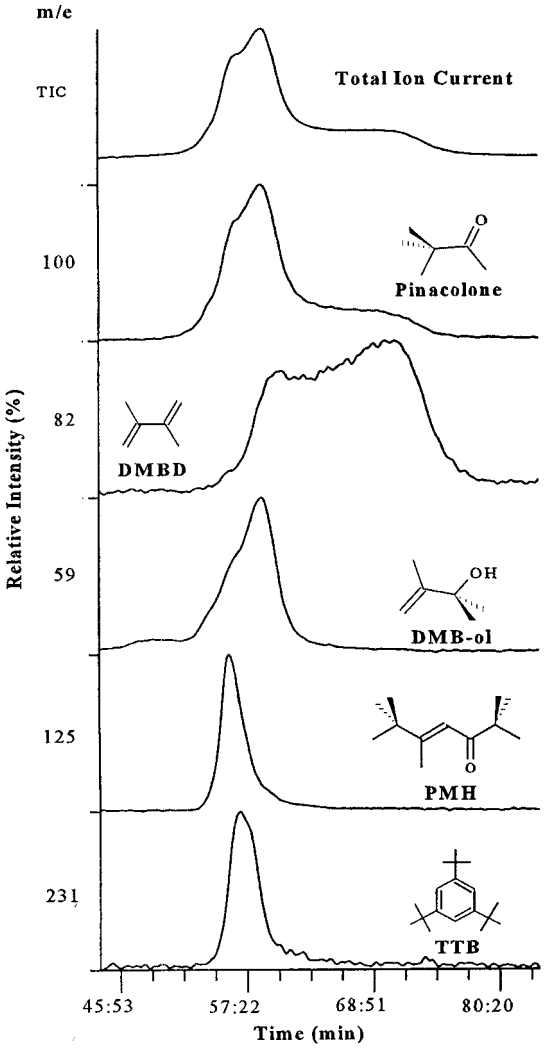

Figure 5. Total ion current and selected ion chromatograms for the organic products of the step II thermal transformation of $Zr_2(OCMe_2CMe_2O)_2(OCMe_2CMe_2OH)_4$ during 7 °C/min heating.

observed. This is the lowest temperature at which thermolysis of the compound takes place and is similar or slightly less than temperatures reported for the thermal transformations of several titanium[10] (550−700 °C) and zirconium alkoxides[8a,b] (220−400 °C). Under the conditions mentioned above, as well as all others employed, the TGA profile possessed three distinct regions: the initial transition (step I) and a second

transition that appears to have two stages (steps IIA and IIB). These stages (IIA and IIB) are separated by a significant change in the rate of transformation wherein the process seems to slow.

Between steps I and II, there is a sufficient plateau period such that separation of the volatiles evolved in step I alone can be accomplished. Careful temperature control of the transformation carried out in a double-chamber Schlenk flask under dynamic vacuum allowed for the separation of the organics given off in step I from those in step II. GC−MS and ^{1}H NMR revealed the sole organic product evolved from 20 to 200 °C (step I terminates ∼210−220 °C) to be pinacol. Likewise, by leaving the transformation flask open to dynamic vacuum for the duration of the first thermolysis step (room temperature to 210 °C), the products for step II can then be trapped free from the step I organic volatiles. Characterization of the trapped step II organics by GC−MS revealed six products (220−270 °C): 2,3-dimethyl-2-butene, 2,3-dimethylbutadiene (DMBD), pinacolone, 2,3-dimethyl-3-buten-2-ol (DMB-ol), 2,2,5,6,6-pentamethyl-4-hepten-3-one (PMH),[17] and 1,3,5-tri-*tert*-butylbenzene (TTB).

In an effort to establish a more exact time of formation for each of the compounds during step II, the thermal transformation was carried out in a mass spectrometer equipped with a variable-temperature probe. Figure 4 shows the total ion current (TIC) for the entire thermolysis (steps I and II) as well as $m/e = 103$, which signifies the evolution of pinacol. From Figure 4, it is clear that pinacol is not a detectable product in step II. The time evolution for each organic product in step II was ascertained by plotting individual ion chromatograms (Figure 5). The selection criteria for the ions were uniqueness to a single compound together with acceptable intensity of the ion. Data in Figure 5 reveal that pinacolone is evolved continuously during step II, while DMB-ol, PMH, and TTB are generated almost exclusively during the first half of step II (step IIA), and that there is a short induction period before the evolution of DMBD. This latter observation is not surprising, as DMBD is the dehydration product of pinacolone and it is known that ZrO_2 can act as a dehydration catalyst.[8] Thus, as the amount of ZrO_2 (catalyst) increases, the rate of the dehydration increases.

Quantification of Volatiles. The large number of products complicated quantification; however, the evolution of 2 equiv of pinacol per dinuclear unit allowed for a convenient check of the method employed for this purpose. The thermolysis was carried out in a manner similar to that described by Girolami et al., with a few modifications.[11] The precursor was heated to 280 °C under static vacuum and all volatiles (from steps I and II) were trapped in the chamber cooled to 77 K. Quantification of the organics was accomplished by ^{1}H NMR using hexamethylbenzene as an internal standard. The error of this procedure was determined by comparing the amount of pinacol expected (based on the amount of sample weighed out) to the amount of pinacol found (based on the internal standard C_6Me_6) and was established to be 7%. Percentages of ligand from $Zr_2(OCMe_2CMe_2O)(OCMe_2CMe_2OH)_4$ consumed to form each C_6 product were found to be pinacol, 33%; pinacolone, 36%; DMBD, 19%; and DMB-ol, 11%. The percentages were based on the normalization of the amount of pinacol to 33%. There was no NMR evidence for the presence of either PMH or TTB. The total thermolysis of $Zr_2(OCMe_2CMe_2O)(OCMe_2CMe_2OH)_4$ is summarized in eqs 1 (step I) and 2 (step II) below.

$$Zr_2(OCMe_2CMe_2O)_2(OCMe_2CMe_2OH)_4 \rightarrow Zr_2(OCMe_2CMe_2O)_4 + 2HOCMe_2CMe_2OH \quad (1)$$

$$Zr_2(OCMe_2CMe_2O)_4 \rightarrow 2.2(\text{pinacolone}) + 1.1(\text{DMBD}) + 0.67(\text{DMB-ol}) + \text{trace PMH} + \text{trace TTB} \quad (2)$$

From the total amount of ligand consumed to form the C_6 products, 99%, it is apparent that very little ligand is converted to the C_{12} and C_{18} species. This observation can be reasonably explained using purely entropic arguments. More specifically, typical thermolysis reaction conditions (low pressure and high temperatures) should disfavor pathways involving bi- or trimolecular reactions.

Mechanistic Studies. Previous thermolysis studies involving titanium and zirconium alkoxides have reported the evolution of aldehydes ($Ti(OEt)_4$), ketones ($Ti(O^iPr)_4$), ethers (both $Ti(OEt)_4$ and $Ti(O^iPr)_4$), olefins, and alcohols ($Ti(OEt)_4$; $Ti(OR)_4$, R = Et, ^{i}Pr, ^{t}Bu; $Zr(OR)_4$, R = ^{i}Pr, ^{t}Bu, $CHCMe_3$).[8a,b,10] These previous reports largely follow the path proposed by Bradley et al.,[8b] which is summarized in the following equation (eq 3).

$$M[OCR(CR''_2R''')R']_4 \rightarrow MO_2 + xHOCR(CR''_2R''')R' + y(\text{olefin}) \quad (3)$$

M = Ti, Zr

R, R′, R″, R‴ = H or alkyl (at least one H)

In most cases, $y > x$ because the alcohol produced can be dehydrated by the metal oxide as the reaction proceeds (eq 4).

$$\text{alcohol} \rightarrow H_2O + \text{olefin} \quad (4)$$

On the basis of eq 3, the major products expected from the thermolysis of zirconium pinacolate would be pinacol and 2,3-dimethyl-2-butene. As has already been stated, very little 2,3-dimethyl-2-butene is produced; therefore, this pathway is not favored. However, the byproduct DMB-ol possesses both the alcohol and olefin functionalities (1:1) and, as such, may be formed by a process similar to that which is theorized for the more traditional group IV alkoxides.[8a,10] The formation of PMH, a C_{12} species, and TTB, a C_{18} compound, is somewhat surprising, as C−C bond formation has not been reported in the thermal transformations of typical zirconium alkoxides and only the ethers formed in previous studies involved any ligand coupling. Although coupling reactions have not been observed in the earlier studies, this type of thermal behavior is not unprecedented for pinacolone (one of the major products) under basic or reducing conditions. Reduction of pinacolone with

(17) Both the trans and cis isomers are produced and are easily separated in subsequent GC−MS studies. The trans isomer is formed in much greater yield, and for the purpose of simplification, all future studies will involve only this structural isomer.

Scheme 1

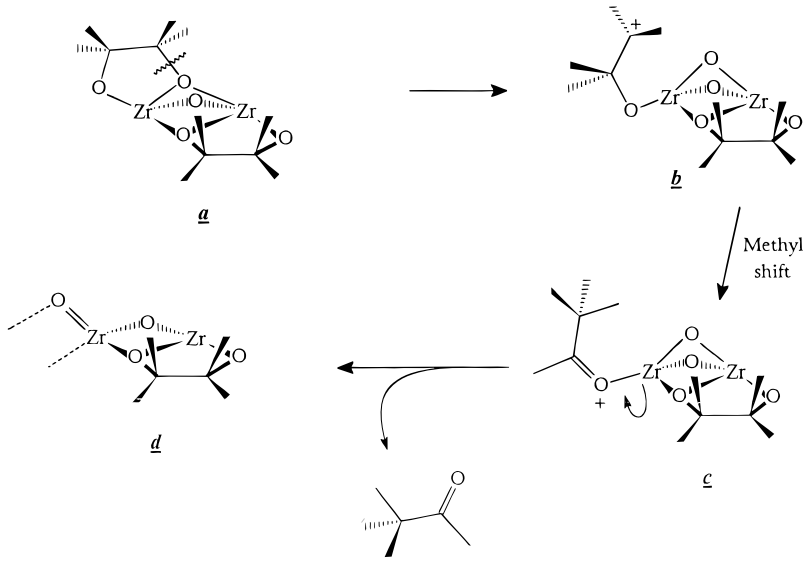

sodium yields several products, including TTB, while reaction of pinacolone with KO^{t}Bu at elevated temperature yields PMH as the major product.[18]

Step I. Formation of Pinacol. The lowest energy process in the pyrolysis of $Zr_2(OCMe_2CMe_2O)_2(OCMe_2CMe_2OH)_4$ involves proton transfer, followed by cleavage of Zr−OH bonds. Initial loss of alcohol is not surprising, as it is also observed to be the first event during heating of $Zr_2(O^iPr)_8(HO^iPr)_2$.[8a] Likewise, the cerium and hafnium analogues will lose their coordinated ^{i}PrOH under even milder conditions by slurrying in CH_3CN or recrystallization from cyclohexane, respectively.[19] Examination of the weight loss observed in the TGA suggests that 2 equiv of pinacol are lost per dinuclear unit, with close agreement for the observed (26%) and calculated (26.8%) values. Since the evolution of 2 equiv of pinacol per molecule corresponds to the removal of all the hydroxyl protons, the intermediate must now contain only doubly deprotonated ligands: it is $[Zr_2(OCMe_2CMe_2O)_4]_n$. Attempts to dissolve this intermediate in Lewis basic solvents such as refluxing tetrahydrofuran (THF) and dimethyl sulfoxide were unsuccessful, suggesting that the material is oligomeric or polymeric. However, the material could be dissolved by refluxing in neat pinacol or very concentrated solutions of pinacol in toluene. ^{1}H NMR revealed the resultant metal-containing species to be mostly $Zr_2(OCMe_2CMe_2O)_2(OCMe_2CMe_2OH)_4$ (a small amount of hydrolyzed material is also present), thus illustrating the reversibility of step I.

Step II. Catalytic Transformation of Pinacolone by ZrO_2. In an effort to establish what, if any, catalytic processes were promoted by the metal oxide, freshly prepared ZrO_2 (from the decomposition of $Zr_2(OCMe_2CMe_2O)_2(OCMe_2CMe_2OH)_4$) and pinacolone (the major organic product in step II) were placed in a tube which was then sealed and heated to 270 °C for a period of 30 min. This experiment was carried out to establish the ability of this metal oxide to carry out the observed transformations as secondary reactions. GC−MS analysis of the liquid phase following heat treatment revealed the presence of PMH and TTB but DMB-ol was not observed. This experiment confirms that ZrO_2 can catalyze the aldol condensation and aromatization of pinacolone and imparts feasibility to the "secondary" mechanism for the formation of PMH and TTB. Since the reaction conditions were so much more vigorous (high pressure vs vacuum) than those present during the typical solid-state thermal transformation, the same test was carried out using a tube furnace to replicate the low pressure and short contact time. $Zr_2(OCMe_2CMe_2O)_2(OCMe_2CMe_2OH)_4$ was first decomposed in the furnace and then pinacolone was subsequently allowed to travel over the freshly prepared oxide and the volatiles were collected in a cold trap. Results obtained by GC−MS agreed with those obtained for the sealed tube experiment.

Formation of Pinacolone. A mechanism for the formation of pinacolone can be suggested (Scheme 1) which is analogous to the well-known pinacolone rearrangement in organic chemistry. Carbon−oxygen bond cleavage is the first step and results in the formation of a carbocation (species **b**). A methyl migration follows, producing a metal-bound ketone where the positive charge has now been transferred to the oxygen (species **c**). Cleavage of the metal−oxygen dative bond gives free pinacolone. In the traditional dehydration of pinacol, a strong acid is used to protonate the alcohol oxygen and form a good leaving group, H_2O. However, in the case of the thermolysis intermediate, $[Zr_2(OCMe_2CMe_2O)_4]_n$, the oxygens are likely bridging two electron-withdrawing Zr(IV), which serve the same role as the protons.

Formation of DMB-ol. Because DMB-ol was not formed in either of the ZrO_2/pinacolone catalysis experiments, a secondary reaction seems unlikely, suggesting that it is a primary product. Three possible primary routes can be envisioned, two of which involve a single ligand (unimolecular) and one which employes a ligand−ligand interaction (bimolecular). Since the production of DMB-ol disappears in step IIB, a necessary ligand−ligand interaction which is diminished by "site isolation" seems a reasonable process as compared to the single-

(18) Bartlett, P. D.; Roha, M.; Stiles, M. R. *J. Am. Chem.. Soc.* **1954**, *72*, 2349−2353.

Scheme 2

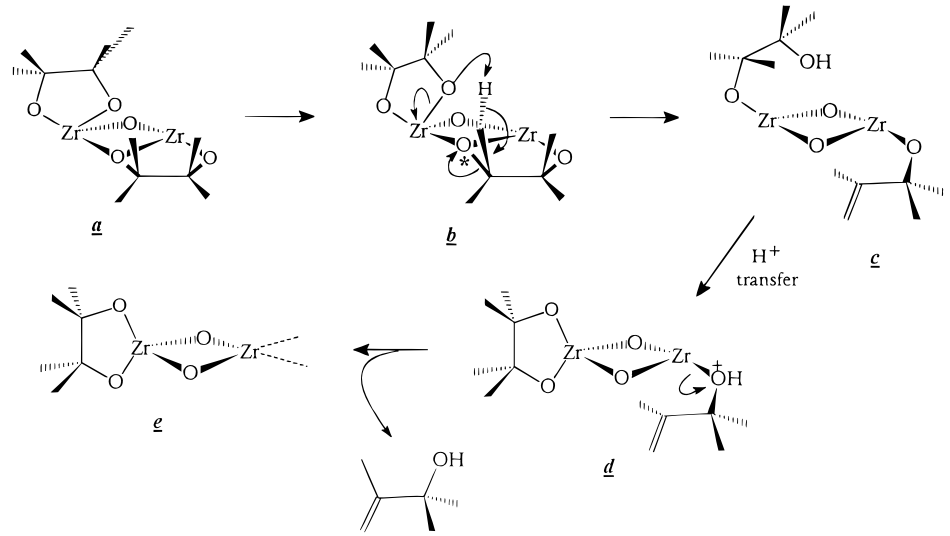

ligand routes. However, it is possible that when metal oxide formation has progressed sufficiently, it catalyzes the dehydration of DMB-ol to the extent that it is no longer observed. As the present data cannot fully rule out this possibility, both the unimolecular and bimolecular processes must be considered and will be presented.

Scheme 2 illustrates the bimolecular mechanism for the formation of DMB-ol. This is a primary process as the C_6 fragment remains covalently bound to the metal prior to release as DMB-ol. Species **b**, shows a concerted step wherein the oxygen of one ligand deprotonates a methyl group from a second neighboring ligand to ultimately give a pendant hydroxyl and olefin, respectively (species **c**). Proton transfer from the pendant hydroxyl to the covalently bound oxygen of the now olefinic ligand (species **d**) leads to the evolution of DMB-ol. A similar unimolecular process is also possible. However, the concerted step illustrated in species **b** now requires that the attacking oxygen and the deprotonated methyl originate from the same ligand. The second possible unimolecular process involves initial C−O bond cleavage as seen in the formation of pinacolone (Scheme 1). Intramolecular proton transfer from a methyl group of the cationic species in **b** (Scheme 1) to the covalently bound oxygen results in the evolution of DMB-ol.

Formation of DMBD. As previously discussed, PMH almost certainly arises from a secondary reaction dehydration of pinacolone with the metal-oxo species. As with DMB-ol, a supplementary operative mechanism (primary in this case) cannot be completely negated. However, persuasive support for the secondary mechanism is found in Figure 5, which shows an obvious induction period for the formation of DMBD. This is consistent with the need for a partial conversion to the metal oxide, which can then act as a dehydration catalyst. Additionally, the evolution of DMBD does not tail off as quickly, also consistent with a secondary mechanism, and can be explained as the result of a steady increase in catalyst, which effectively compensates for the decrease in substrate (pinacolone).

Formation of PMH and TTB. The C_{12} and C_{18} species (PMH and TTB) must arise from ligand-coupling reactions, and their formation in step IIA and subsequent disappearance in step IIB can be explained by either of two possible mechanisms. In a "primary" mechanism, the ligands couple while still covalently bound to the metal. When the conversion has proceeded to the extent that the ligands reach a condition of "site isolation", the coupling stops. Alternatively, an argument can be made for a "secondary" reaction (evolved C_6 fragments interact with the metal/oxo/alkoxo material) in which PMH and TTB are formed by the metal-oxo-mediated aldol condensation or cyclization of previously formed pinacolone (respectively). Finally, when the vapor pressure of the pinacolone drops to a sufficiently low level, this reaction pathway becomes negligible. In previously discussed experiments, it was shown that PMH and TTB could be formed by a secondary pathway involving pinacolone and ZrO_2. Since this does not rule out the possibility of an active primary mechanism, we sought independent verification for the presence and/or absence of both mechanisms.

Scheme 3

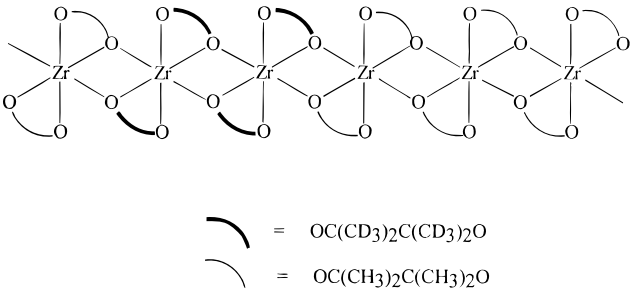

To establish the operative mechanism (primary, secondary, or both), a labeling experiment was designed. This necessitated the preparation of $Zr_2(OCMe_2CMe_2O)(OCMe_2CMe_2OH)_4$-$d_{72}$, wherein all the methyl groups were fully deuterated. Next, the fully deuterated and undeuterated dinuclear complexes were mixed in a 1:3 or 1:4 ratio, respectively. The resulting solid mixture was dissolved briefly (~20 min total) to ensure molecular mixing and the solvent removed in vacuo. Subsequent pyrolysis of the material and partial quantification of the organic products by GC−MS completed the experiment. It was hoped that the isotopomer ratios of one of the ligand-coupled products (PMH, in this case)

would allow for a conclusion about its formation. By choosing a 1:3 or 1:4 ratio (fully deuterated:fully undeuterated zirconium pinacolate), the expected PMH isotopomer ratios should differ significantly.

If a *secondary* mechanism is operative, the ratio of PMH isotopomers should be purely statistical, given by the multipliers of X, Y, and Z in eq 5.

$$m^2X + 2mnY + n^2Z = 1 \quad (5)$$

m = the mole fraction of deuterated pinacolone

n = the mole fraction of undeuterated pinacolone

X = the fraction of PMH-d_{22} formed

Y = the fraction of PMH-d_{10} or -d_{12} formed

Z = the fraction of PMH-d_0 formed

If, however, a *primary* mechanism is at work, the relative abundance of fully deuterated and half-deuterated PMH should be higher than statistical expectations because, regardless of the value of m, the deuterated ligand is in relatively high "local" concentration (see Scheme 3). This arises from the fact that the metal centers come in groups of two (no randomization), each possessing their original ligand sets. Although the structure of the intermediate is not known, any possible structure of the resulting polymeric material should have a similar high local concentration of the deuterated ligand. For the polymer shown here (Scheme 3), each deuterated ligand has an equal chance to couple with a second deuterated ligand or a nondeuterated ligand. This results in statistically even amounts of d_{12}-ligand contributing to PMH-d_{22} and PMH-d_{10} or -d_{12} for a primary mechanism. Thus, the largest ratio of X:Y should always be 1:2.[20]

$$(^1/_2m)X + mY + (n - {}^1/_2m)Z = 1$$

For a valid interpretation of experimental results, a few conditions must be met. First, the brief dissolution of the deuterated and nondeuterated compounds, which ensures molecular mixing of the intact isotopomers, must not effect ligand transfer between dinuclear units; that is, no partially deuterated complexes (e.g., $Zr_2(OC(CD_3)_2C(CD_3)_2O)_2(OC(CH_3)_2C(CH_3)_2OH)_4$-$d_{24}$ can be formed. Second, in losing the first 2 equiv of pinacol, step I, the initial dinuclear units cannot be broken up. Stated another way, this also means that the two metal ions which are bound to each other in the dinuclear complex are still adjacent to one another in the polymer formed during the thermal transition of step I, yielding an intermediate similar to that illustrated in Scheme 3.

To ensure that no ligand exchange occurred during dissolution of the two compounds, an experiment was carried out using $Zr_2(OCMe_2CMe_2O)_2(OCMe_2CMe_2OH)_4$-$d_{72}$ and unlabeled pinacol. The ^{1}H NMR spectrum of the labeled dinuclear complex dissolved in CD_2Cl_2 displayed no appreciable signals in the methyl region. Next, ~3 equiv of pinacol was added and the ^{1}H NMR measured again. Once again, no appreciable signals in the ligated methyl region except that for free pinacol were observed. The NMR was measured again after 1 h with no noticeable change. Since no significant amount of unlabeled "free" pinacol is incorporated into the dinuclear complex over the course of 1 h, ligand scrambling *between* complexes, which surely must be slower, is not expected to occur in significant proportions.

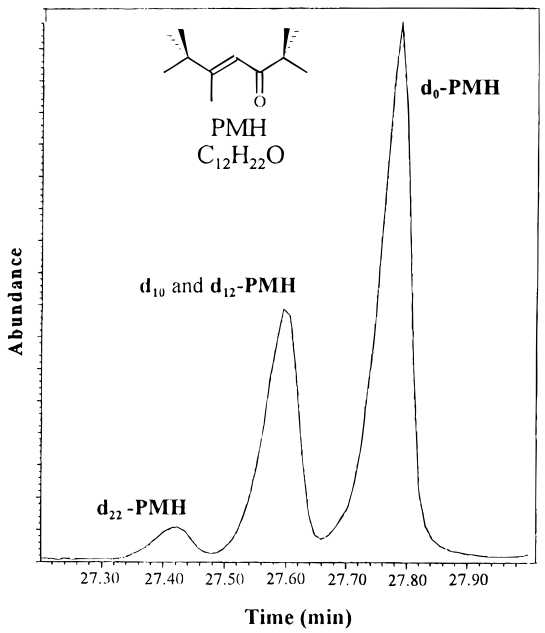

Figure 6. Gas chromatogram of the isotopomers of PMH.

Table 3. Calculated vs Observed PMH Isotopomer Ratios

			expected ratio[b]		
m[a]	n	vacuum	"primary"	"secondary"	observed ratio[c]
0.2	0.8	dynamic	1:2:7	1:8:16	1:7.7:17.8
0.2	0.8	static			1:7.2:17.6
0.25	0.75	dynamic	1:2:5	1:6:9	1:6.4:10.8
0.25	0.75	static			1:6.1:10.3

[a] Values of $m < 0.2$ gave PMH-d_{22} peaks too small to integrate. [b] Ratios were predicted using eqs 3 and 4. [c] Each ratio is the average of three separate injections.

The second condition, while it cannot be proven experimentally, is very likely. The metal ions in the precursor are multiply ligated to each other (see Figure 1); moreover, breaking up these dinuclear units is tantamount to "diffusion" of the metal centers. It is most likely that, in the solid state and at these temperatures (~200 °C), there will be no significant atom rearrangement, including randomization of metal centers. The fact that the initial loss of pinacol is reversible lends further validity to this assumption. An important corollary to this assumption is that the two metal centers in a single dinuclear complex will be adjacent to each other in the polymeric species. It is this fact that will permit mechanistic conclusions based on the ratio of isotopomers produced.

One further possible complication is the presence of a kinetic isotope effect. Because the first step in the formation of PMH involves C−H bond cleavage (see Scheme 2), it was thought that a kinetic isotope effect

(19) Vaartstra, B. A.; Huffman, J. C.; Gradeff, P. S.; Hubert-Pfalzgraf, L. G.; Daran, J.-C.; Parraud, S.; Yunlu, K.; Caulton, K. G. *Inorg. Chem.* **1990**, *29*, 3126−3131.

(20) A more detailed explanation can be found in the Supporting Information.

Scheme 4

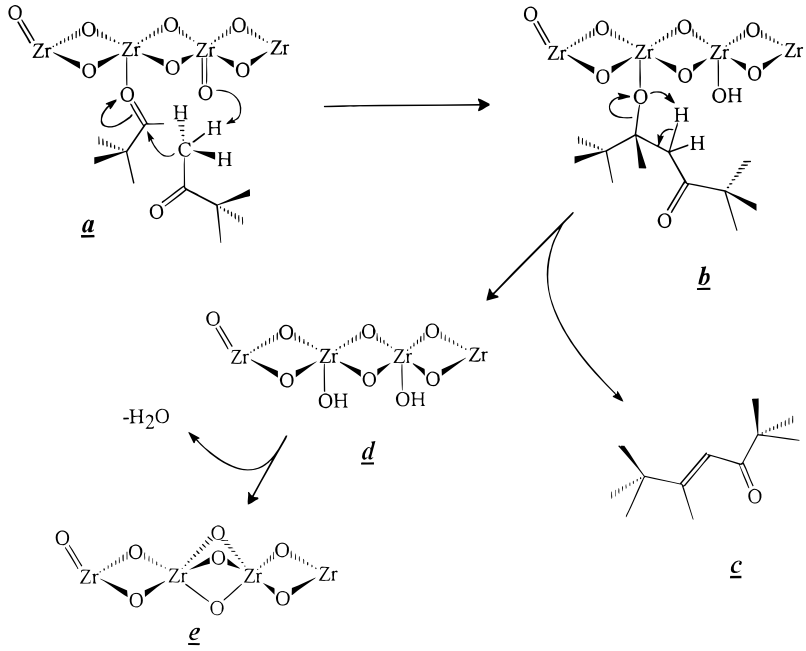

(still significant at 280 °C) would cause a disparity between the expected and observed ratios. However, as will be revealed shortly, there is no observable effect. An explanation for the apparent lack of complication came from inspection of the mass spectra of the deuterated and nondeuterated pinacolone evolved in the experiment. From these spectra, it was apparent that significant isotope scrambling had occurred. While the *tert*-butyl groups remained isotopically pure, the methyl (as seen by the range of molecular ions) of the ketones had been scrambled to the extent of possessing nearly the same (statistical) amount of hydrogen and deuterium, thereby eliminating any isotope effect. Likewise, the mass spectra of the PMH isotopomers revealed isotopically pure *tert*-butyl groups, but a small range of masses (3−4 amu) for the molecular ions. Further control experiments confirmed the necessity of the metal-oxo species for the isotope scrambling observed in pinacolone. This interaction leads to its dehydration to give DMBD and coupling to give PMH and TTB. Furthermore, it must be *reversible*, because pinacolone is the major product in step II, and *rapid*, as it must occur many times (under entropically unfavorable conditions) for the methyl group to become statistically scrambled.

Following these preliminaries, thermolysis of the mixed deuterated and nondeuterated zirconium pinacolate was carried out. Two separate samples (20 mol % and 25 mol % of deuterated Zr pinacolate[21]) were divided in half and thermolyzed both in a tube furnace (dynamic vacuum) and in a double-bottom Schlenk flask (static vacuum), as has already been described. Seen in Figure 6 is a GC−MS chromatogram showing the achieved separation of the PMH isotopomers. Table 3 lists the results of the GC−MS analyses from the four separate thermolyses, and from these numbers it is apparent that a secondary mechanism is operative.

(21) Smaller amounts of the deuterated complex did not yield sufficient PMH for integration by GC−MS.

Scheme 4 illustrates the proposed secondary mechanism for the formation of PMH by the coupling of pinacolone. In the first step, **a**, a metal-bound oxide pulls a proton from the ketone methyl, rendering that carbon more nucleophilic. At the same time, the oxygen of a second ketone binds datively to a metal center, making the carbonyl carbon more electrophilic. If oriented correctly, the nucleophilic carbon of one molecule can attack the electrophilic carbon of a second and form a new C−C bond. Proton transfer from the methylene group to the ether oxygen results in the formation of a C−C double bond and evolution of free PMH (**b** and **c**). Finally, release of the H_2O abstracted from the ligands regenerates the metal oxide (**d** and **e**). Although the mechanism of formation of TTB may not be identical to that for PMH, we believe the results seen for the isotope studies involving PMH can be applied to TTB and that both C_{12} and C_{18} compounds arise from the coupling of "free" pinacolone, which is mediated by the zirconium-oxo species.

Conclusions

The use of a chelating alcohol can have a dramatic effect on the physical properties of the corresponding metal alkoxide. A reduction of volatility and solubility is observed upon the substitution of pinacol for 2-propanol in the starting compound, $Zr_2(O^iPr)_8(HO^iPr)_2$. This loss of volatility resulted in the employment of bulk thermolysis as the most convenient method with which to probe the thermal reactivity of the compound $Zr_2(OCMe_2CMe_2O)_2(OCMe_2CMe_2OH)_4$. However, the nonvolatile nature of the alkoxide allowed for the utilization of a variable-temperature mass spectrometry experiment, resulting in the real-time examination of the decomposition. From the studies herein, it appears that there are two primary mechanisms for the decomposition of zirconium pinacolate. These give rise to pinacolone and DMB-ol following liberation of pinacol. The mechanism proposed for the formation of DMB-ol is analogous to mechanisms generally accepted for

thermolysis of early transition metal alkoxides (giving ROH and olefin). Ketones have been seen previously but have never been a major product, as is found here. Thus, the pinacolate has at its disposal both the traditional pathway and an additional more energetically favorable (based on the yield of pinacolone) pathway to oxide. The latter clearly derives from the structure of the pinacol backbone, in which methyl migration facilitates C−O bond heterolysis. Thus, established organic chemical reactivity can favorably influence thermolysis behavior.

Acknowledgment. This work was supported by the Department of Energy.

Supporting Information Available: An explanation for the observed ^{1}H NMR and expected isotopomer ratios (3 pages). Ordering information is given on any current masthead page.

CM970644E